Am J Transl Res 2020;12(11):7312-7325
www.ajtr.org /ISSN:1943-8141/AJTR0104164

Original Article

Effects of injectable platelet rich fibrin on bone remodeling in combination with DBBM in maxillary sinus elevation: a randomized preclinical study

Zhixiang Mu[1,2*], Qingqing He[1*], Liangjing Xin[1], Yihan Li[1], Shuai Yuan[1], Huawei Zou[1], Linjing Shu[1], Jinlin Song[1], Yuanding Huang[1], Tao Chen[1]

[1]*Stomatological Hospital of Chongqing Medical University, Chongqing Key Laboratory of Oral Diseases and Biomedical Sciences, Chongqing Municipal Key Laboratory of Oral Biomedical Engineering of Higher Education, Chongqing 401147, China;* [2]*Department of Periodontics, School and Hospital of Stomatology, Wenzhou Medical University, Wenzhou 325027, Zhejiang, China.* [*]*Equal contributors.*

Received October 29, 2019; Accepted October 9, 2020; Epub November 15, 2020; Published November 30, 2020

Abstract: Objectives: This study aims to assess the angiogenic and osteogenic capacity in rabbit sinus model grafted with Deproteinized bovine bone mineral (DBBM) particles soaked in injectable Platelet rich fibrin (iPRF), both of which interacted to form an integrated block. Materials and methods: Among sixteen rabbits, bilateral maxillary sinuses were randomly grafted with either DBBM containing iPRF (iPRF+DBBM group), or DBBM alone (DBBM group). After a 4 and 8-week healing period, animals were sacrificed for micro-CT, histological and immunofluorescence analyses, respectively. Results: New bone formation in the iPRF+DBBM group was largely observed around the basal bone wall and Schneiderian membrane (SM), which further substitute the bone grafting material in a bidirectional remodeling pattern. Although the ultimate amount of bone volume was of no significant difference between two groups in radiographical image, the expression of ALP and TRAP staining were significantly higher in the experimental group with numerous vascular formations at 4th week. Moreover, the substitution rate of DBBM by new bone formation after 8 weeks was significantly higher in the experimental group. As a result, mature collagen fibers were detected in the larger amount of area in iPRF+DBBM group even at an early stage. Conclusion: iPRF+DBBM accelerated vascular formation, bone remodeling and substitution of bone graft materials at the early healing period, even though it failed to increase the bone volume in a long-term period. This integrated grafting biomaterial will have great potential in the application of sinus augmentation, which provides a favorable environment for early implant placement.

Keywords: Sinus floor augmentation, platelet, dental implant, bone substitutes, animal study

Introduction

The posterior maxillary region is faced with multiple challenges during implant placement due to poor bone quality and bone resorption caused by sinus pneumatization after tooth loss and inflammatory disease [1, 2]. Among a multiple of therapeutic approaches, sinus floor augmentation (SFA) procedure is the most commonly used approach to provide sufficient bone volume for further implant placement [3]. Although assorted bone grafting materials, including autogenous bone, allogeneic bone and xenografts, are currently applied for SFA, these grafting materials have drawbacks, including limited donor availability, donor site morbidity, disease transmission and immunogenic response [4]. As a result, many biocompatible materials have been fabricated as a substitute to traditional graft materials.

Deproteinized bovine bone mineral (DBBM) appeared as one of the most popular employed xenografts, which are biocompatible materials commonly chose for SFA [5]. Most of the studies have reported successful outcomes both in histological and clinical perspectives [3, 6]. However, DBBM, possessing only the ability of osteoconduction but no osteoinduction and osteogenesis due to the absence of the biological factors, cannot activate new bone regeneration by itself [6]. Moreover, with a rather pro-

longed degradation rate, DBBM usually retards the replacement of new bone formation and prolongs the graft-healing time, and fails to synchronize with the osteogenic rate. Hence, combining the graft material with a biologic promoter that contains crucial growth factors may reduce the graft-healing time and enhance the osteoinductive process of bone remodeling.

To make up for the lack of osteoinductive and angiogenic capacity and further promote bone regeneration, the utilization of exogenous growth factor is developed, such like vascular endothelial growth factor (VEGF) and recombinant human platelet derived growth factor-BB (PDGF-BB) [7]. However, the use of exogenous growth factors costs high and has some inevitable side effects, including excessive inflammation response, heterotopic ossification and carcinogenic effect [8, 9]. Therefore, the attempt to fabricate autologous blood derivatives, with a proven biological safety and simple procedure, has grabbed a mass of attention for SFA recently.

Autologous blood derivatives were obtained after processing a whole blood sample through centrifugation [10]. Notably, the development of the low speed centrifugation concept promoted the creation of a new formulation of platelet-rich fibrin (PRF), namely iPRF [11]. This is a liquid formulation obtained for injectable purpose. iPRF does not consist of any anticoagulants and can maintain in liquid state for about 15 minutes after centrifugation. iPRF bears an extra benefit of aggregating into a fibrin clot shortly after injection [11, 12]. This bio-active material contains PDGF, VEGF, transforming growth factor-β (TGF-β) and so on [12]. These growth factors play a vital role in cell migration, proliferation, and vascularization for tissue regeneration.

However, the therapeutic effect of autologous blood derivatives in bone regeneration is remained obscure. According to the 5th consensus statement of European Association for Ossointegration (EAO), the application of PRF and PRP in SFA together with grafting materials is not advisable due to a lack of effect [13]. However, some studies proposed short-term improvement on outcome evaluation related to osteogenesis and densitometric values [6]. Moreover, numerous previous experimental studies in vitro and in vivo have also supported that combination application of autologous blood derivatives with bone grafting material can promote bone regeneration especially in early healing period [14-16].

To this end, DBBM with iPRF were mixed attempting to accelerate bone remodeling with properties greater than what they can accomplish respectively. Therefore, this study was carried out to assess the angiogenesis and osteogenesis using Bio-Oss particles (A common commercial DBBM) incorporated with iPRF in a rabbit sinus model. Different from previous research, multiple approaches including radiographic and histological analyses were applied to illustrate the efficacy and dynamic pattern of bone regeneration during the early healing stage. We hypothesized that, as a desirable carrier for bioactive factor delivery, grafting the maxillary sinus with iPRF+DBBM may be considered as a candidate treatment for future SFA due to its rapid angiogenesis, faster bone remodeling, cost-efficiency and tissue regeneration capacity, thus allowing earlier implant treatment.

Materials and methods

Materials preparation

For iPRF preparation, the centrifugation process was performed according to the previous method [12]. 1 ml upper layer of transparent pale-yellow sticky liquid in the test tube was collected as iPRF. 0.5 g DBBM (Bio-Oss, Geistlich Pharma AG, Wolhusen, Switzerland) and 1 ml iPRF were mixed together as iPRF+DBBM.

Stereomicroscope and scanning electron microscope (SEM)

The morphology of DBBM and iPRF+DBBM was observed by stereomicroscope (SteREODiscovery V20, Carl Zeiss, Germany). Afterwards, iPRF, DBBM and iPRF+DBBM were frozen at -80°C, followed by freeze-drying to remove water. The cross-section of the materials was sprayed with gold for 120 s and the microstructure of them was observed by SEM (FEI, Quanta 450, USA).

Enzyme-linked immunosorbent assay (ELISA)

In order to detect the amount of released growth factors from iPRF group (200 ul iPRF) and iPRF+DBBM group (200 ul iPRF + 0.1 g

DBBM), the above samples were soaked in 1 ml PBS and then placed on the shaker (30 r/minute) under 37°C. 1 ml of PBS supernatant was extracted at 1 d, 3 d, 6 d, 10 d, and 14 d respectively, and equivalent amount of fresh PBS was added afterwards. According to the previous protocol, the amount of PDGF-BB, VEGF and TGF-β were detected at each time point using ELISA kit. All experiments were carried out in triplicate, with three samples in each group.

Cell culture

Pre-osteoblasts MC3T3-E1 (3111C0001CCC000012, Chinese Academy of Medical Sciences, China) were incubated in α-MEM supplemented with 1% penicillin-streptomycin and 10% FBS. The human umbilical vein endothelial cells line (HUVECs, 3111C0001CCC000437, Chinese Academy of Medical Sciences, China) were cultured in Dulbecco's Modified Eagle's Medium (DMEM) supplemented with 1% penicillin-streptomycin and 20% FBS. Incubation of the first 10 passages of HUVECs was utilized for the following experiments.

Migration assay

The migration assay was implemented following the previous protocol [17]. 0.5 g DBBM (DBBM Group) and 1 ml iPRF + 0.5 g DBBM (iPRF+DBBM Group) were cultured in 5 ml α-MEM, respectively. The supernatant was collected after 1-day culture, which was used to prepare 20% conditioned medium.

The assay was implemented with polyethylene terephthalate cell culture insert (Costar, Corning Inc., Corning, NY, USA) and its pore size is 8 um. The conditioned medium was added into the lower chamber. After starving for 12 h, 1×10^4 cells were resuspended and seeded into the upper chamber and began to migrate. 24 h later, all the samples were treated with 4% formaldehyde (PFA) and then stained with 0.1% crystal violet solution (GoodBio Technology Co., Wuhan, China) for 10 min. The upper chamber of the membrane was rinsed and the cell debris on the top of the membranes was removed by a cotton swab. Optical microscope (Carl Zeiss, Germany) was used to capture images on the bottom of the inserts. All the experiments were performed in triplicates with three specimens in each group.

Tube formation assay

0.5 g DBBM (DBBM Group) and 1 ml iPRF + 0.5 g DBBM (iPRF+DBBM Group) were cultured in 5 ml DMEM, respectively. The supernatant was collected after 1-day culture, which was used to prepare 20% conditioned medium. Tube formation assay was conducted to investigate the angiogenic impact of the above two conditioned media on HUVECs. 2×10^5 HUVECs were seeded into 24-well plates pre-coated with Matrigel and incubated for 4 hours under conditioned media. ImageJ 8.0 software (NIH, Bethesda, MD, USA) was used to count the number of nodes, branches and total branches length.

Quantitative reverse transcription-polymerase chain reaction (qRT-PCR)

Total RNA was harvested at 1 day to investigate the mRNA levels of *VEGF, Col-1 and Ang-1.* Briefly, 2×10^5 cells were seeded into 12-well plates. After 12 hours incubation, DBBM and iPRF+DBBM were added into the medium, respectively. Primer and probe sequences for genes were fabricated with primer sequences according to **Table 1**. The relative mRNA expression level was detected via qRT-PCR according to the previous method [18]. The experiments were performed in triplicate with three samples in each group.

Animals and study design

Sixteen male New Zealand rabbits (3.0 ± 0.5 kg, Animal Center of Chongqing Medical University) were divided into two groups: (1) DBBM group and (2) iPRF+DBBM group (assigned randomly). All experimental procedures, in accordance with the ARRIVE guidelines, were approved by Animal Ethics Committee of Chongqing Medical University (CQHS-IRB-2018-07). The animals were fed separately in cages without limitation of food and water, and temperature was kept at 20-25°C with air humidity reaching 60%-70%.

Surgical procedure

New Zealand rabbits were established as the SFA model as previously reported [18]. Briefly, a sagittal incision was performed along the midline on the dorsal area of the nasal bone, and a full-thickness flap was laterally elevated. Trephine bur was gently utilized to create

Table 1. Characteristics of primers

Cell	Symbol	Forward	Reverse
HUVECs	VEGF	5'-ACCACACCATCACCATCGAC-3'	5'-TTCCGGGCTCGGTGATTTAG-3'
	Ang-1	5'-GAGCAAGTTTTGCGAGAGGC-3'	5'-TGAGTCAGAATGGCAGCGAG-3'
	Col-1	5'-AGTGGTTTGGATGGTGCCAA-3'	5'-GCACCATCATTTCCACGAGC-3'
	GADPH	5'-ACTAGGCGCTCACTGTTCTC-3'	5'-ATCCGTTGACTCCGACCTTC-3'

standard-sized 5-mm-diameter circular windows bilaterally. Subsequently, the Schneiderian membrane (SM) elevated carefully from the basal bone. After the elevation of SM, the lifted cavity was implanted with DBBM (DBBM group) and DBBM combined with iPRF (iPRF+DBBM group), respectively. The implants were then inserted properly. The periosteum and skin were sutured carefully layer by layer with the 4-0 monofilament. The animals were sacrificed with overdose anesthetic. Both maxillary sinuses were removed and immediately immersed in 4% PFA.

Micro-CT

The fixed maxillary sinus samples were imaged by micro-CT (vivaCT80, SCANCO Medical AG, Switzerland). The scanning condition was acquired at 70 kV and 112 μA using a 15.4-μm-thick aluminum filter per slice. Three-dimensional (3D) reconstruction of the interest areas was performed. Bone volume density (BV/TV) and trabecular thickness (Tb.Th) were measured using the built-in software μCT80 (SCANCO Medical AG, Switzerland).

Fluorescence assay and VG staining

For the eight-week group, intramuscular injection of tetracycline (TE, 25 mg/kg), calcein (CA, 25 mg/kg) and alizarin red (AL, 30 mg/kg) were implemented at 2, 4 and 7 weeks postoperatively [4, 11]. These above agents are calcium chelating agents with fluorescence. We injected different fluorescent agents to observe the calcium precipitation in bone tissue [11].

Graded dehydration was then conducted for specimens of the eight-week group. Afterwards, specimens were embedded in methyl methacrylate (M55909) and sliced with Hard Tissue Sawing System (E200CP, EXAKT Verteriebs, Germany) to 50 μm. Then, the fluorescently labeled sections were captured by laser scanning confocal microscope (LSCM) (TCS.SP8, Leica, Germany) to evaluate the bone regeneration at different times. Subsequently, the above samples were stained with VG staining. New bone formation observed beneath the SM was defined as ROI-I and the upper part of the basal bone was defined as ROI-II.

Histological analysis

In addition, the other half of the samples were put in buffered 10% EDTA for the demineralization and embedded in paraffin. The center of these samples was sectioned consecutively into 6 mm thick sections. Slices were then stained with H&E, tartrate-resistant acid phosphatase (TRAP) alkaline phosphatase (ALP) and Masson trichrome (MT). MT staining was conducted to analyze areas of new immature collagen formation (blue color) and areas with matured collagen (red color), distinguishing new bone formation area from mature bone formation area [19].

Immunofluorescence analysis

Immunostaining was carried out according to previous procedures [20]. In short, tissue sections were de-paraffinized following standard procedures and incubated with the primary SDF-1 monoclonal antibody (MAB350, RD) overnight at 4°C. Nuclei were stained with 4, 6-diamidino-2-phenylindole (DAPI). Images were captured by LSCM and the number of immuno-positive cells was counted in the entire area of each photograph.

Histomorphometric analyses

Semi-quantitative analysis was carried out by imageJ v1.8.0 (NIH, MD, USA). At least 4 slides of each sample were used for quantification. Two blinded examiners performed the histomorphometric analysis.

Statistical analysis

All the results obtained from multiple independent experiments are presented as means ±

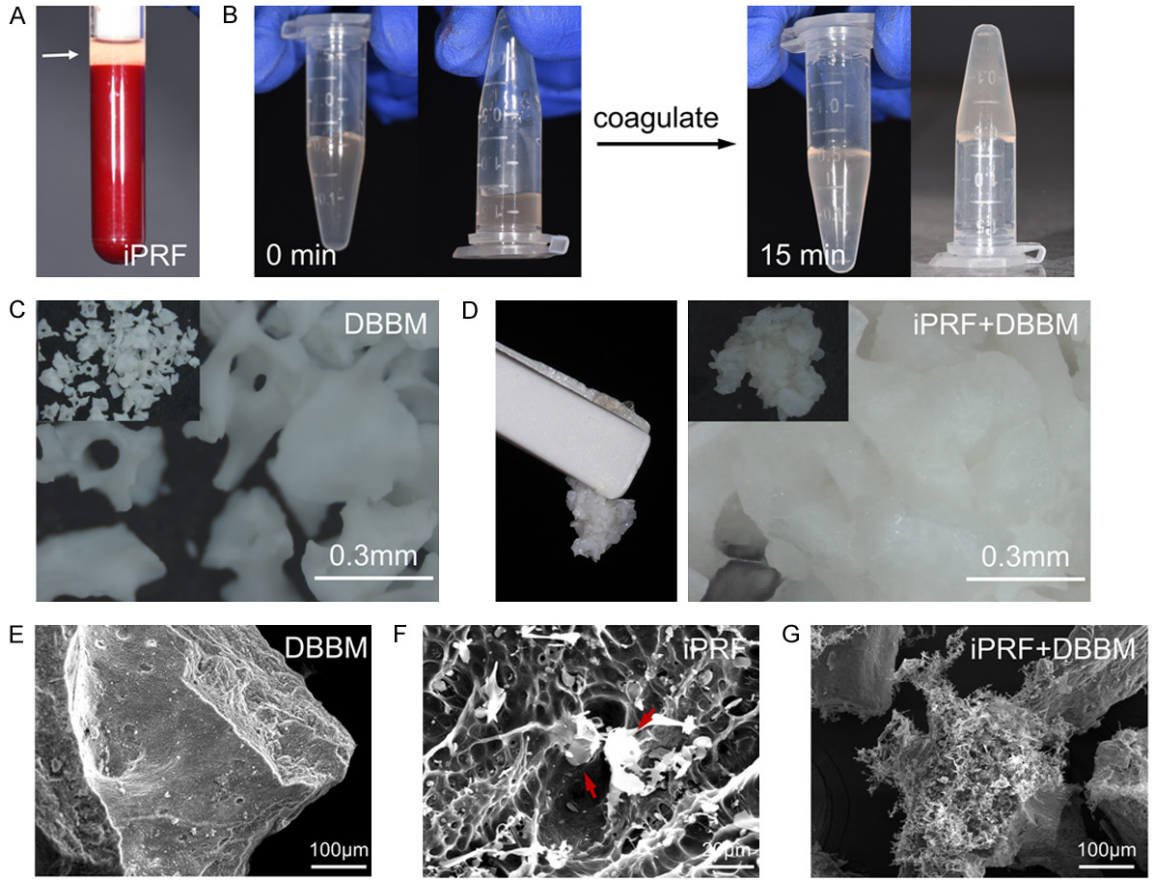

Figure 1. (A) Preparation of injectable platelet rich fibrin (iPRF). White arrow indicates iPRF after centrifugation of blood. (B) The state of iPRF transforms from liquid to fibrin clot only after 15 min. (C, D) Stereomicroscope images of Bio-Oss particles and Bio-Oss particles soaked in iPRF. SEM images of DBBM (E), iPRF (F) and iPRF+DBBM (G) Red arrow indicates leukocytes within iPRF.

standard deviations. The Shapiro-Wilk test was conducted by SPSS Statistics version 20.0 (IBM Corp., Armonk, NY.) to detect the normality of the variables, and all the variables showed normal distribution. Student t tests was used for comparison among different groups. Asterisks represent the gradation of significant differences: $*P < 0.05$; $**P < 0.01$.

Results

Characterization of DBBM and iPRF+DBBM

After the centrifugation step, it was possible to observe subdivisions of the material inside the tube and an obvious iPRF portion (1 ml) at the top of the tube (**Figure 1A**). iPRF maintains a liquid state for around 15 minutes before finally turn into a fibrin clot (**Figure 1B**). Stereomicroscope images showed that DBBM particles are scattered and irregular with porosity (**Figure 1C**). However, after loaded with iPRF, DBBM particles were aggregated and the pores were filled with iPRF (**Figure 1D**). SEM indicated that DBBM combined with iPRF became a fibrin clot as a whole (**Figure 1G**). Leukocytes can be observed on the fibrin network of iPRF (**Figure 1F**).

DBBM degradation and new bone formation

Bone volume around the implant region was imaged by micro-CT in sagittal plane (**Figure 2A**). In addition, bone volume over total volume (BV/TV) and thickness of trabecular bone (Tb.Th) in iPRF+DBBM group increased slightly with no statistical difference to DBBM group (**Figure 2B**, **2C**). As shown in **Figure 2D**, the dynamic pattern of osteogenesis in two groups was analyzed by sequential fluorochrome labels. Compared to DBBM group, iPRF+DBBM group showed faster bone formation during the early

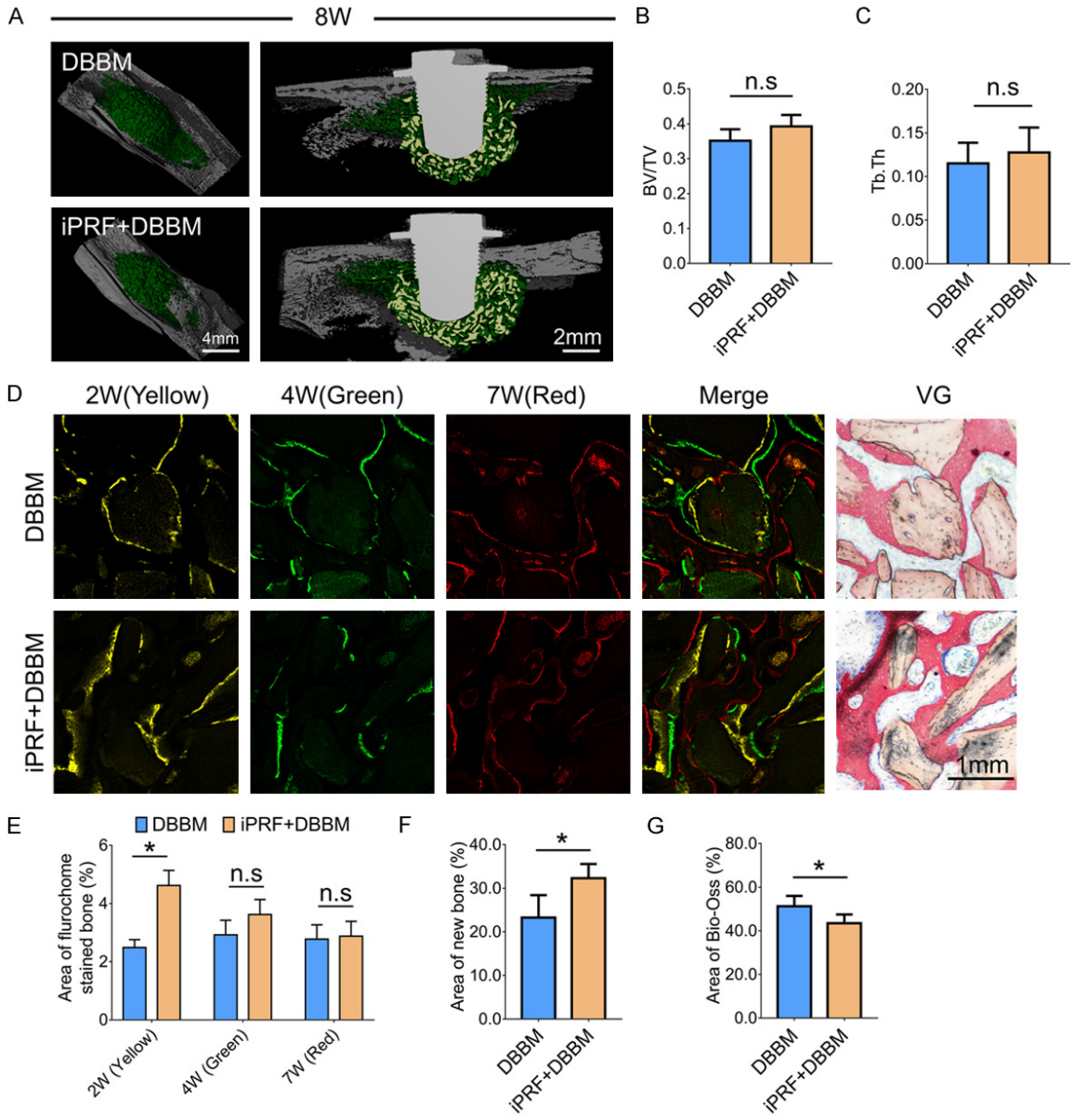

Figure 2. (A) Micro-CT analysis showing 3D reconstruction image of DBBM and iPRF+DBBM group at 8 weeks after sacrifice. (B, C) Bone-related parameters (BV/TV and Tb.Th) in DBBM and iPRF+DBBM groups analyzed by Micro-CT (n = 3). (D) Laser confocal microscope photographs showing the dynamic pattern of osteogenesis in DBBM and iPRF+DBBM groups, together with VG staining of both groups after sacrifice. (E) Semiquantitative analysis of bone formation at 2nd, 4th, 7th week. Semiquantitative analysis of DBBM area (F) and new bone formation rate (G) of DBBM and iPRF+DBBM groups (n = 4). *$P < 0.05$.

healing period (at 2nd week), while there is no significant difference between two groups in the late period (at 7th week) (**Figure 2E**). According to VG staining at 8th week postoperatively, the degradation of DBBM is accelerated in experimental group and the remaining space was substituted by larger amount of new bone (**Figure 2F**, **2G**).

Cell migration and recruitment

VG staining indicated that in both groups, new bone formation was detected beneath the SM and in the upper part of the basal bone, with immature matrix components connecting the two regions (**Figure 3A**). Compared to the DBBM group, iPRF+DBBM group showed that

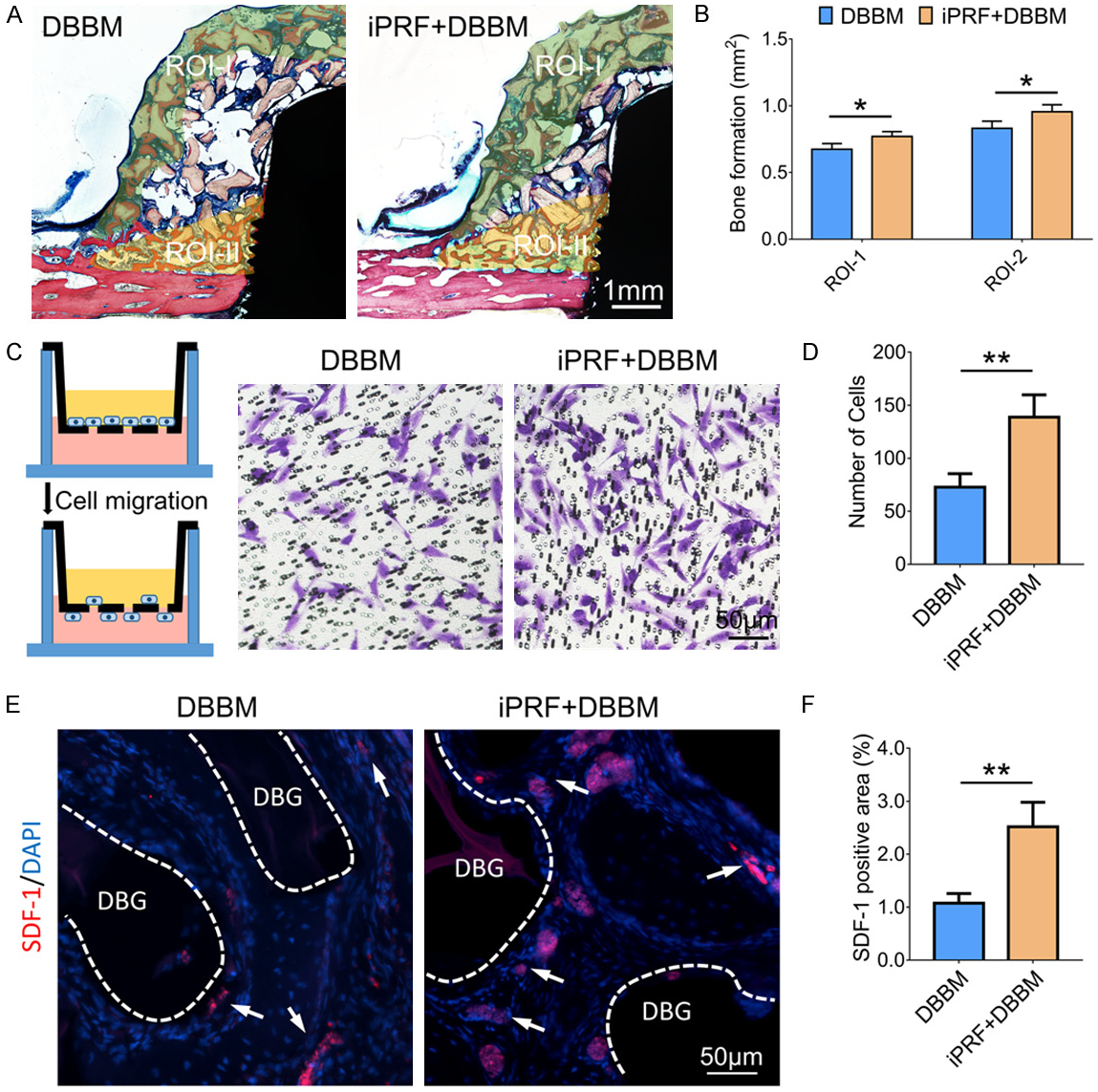

Figure 3. A. VG staining of hard tissue sections showing new bone formation in DBBM and iPRF+DBBM groups at 4 weeks post-operatively. B. Semiquantitative analysis of bone formation in different regions of interest (n = 4). C. A Transwell system and crystal violet staining were used to test migration capacity of MC3T3-E1. D. Semiquantitative analysis of migrating cells in DBBM and iPRF+DBBM groups after 24 h culture (n = 3). E, F. Immunofluorescence staining images and semiquantitative analysis of SDF-1 (n = 4). (DBG: DBBM grafting) $*P < 0.05$, $**P < 0.01$.

new bone formation was mostly detected in the lower part of the SM (ROI-I) and the upper part of the basal bone (ROI-II) (**Figure 3B**). This may be due to the elevated migration of osteoprogenitor cells. Therefore, Transwell assays were performed to analyze their ability to promote cell migration. The results showed that the combination of iPRF and DBBM significantly promoted cell migration, and the number of migrating cells was about twice higher than that of DBBM group (**Figure 3C**, **3D**). This migration can be mediated by chemokines. Stromal cell-derived factor-1 (SDF-1) has been recognized as the most important chemokine for cell recruitment and homing [21]. Therefore, the expression level of SDF-1 protein was analyzed to investigate the effects of two groups on cell migration. Immunofluorescent outcome indicated that expression of SDF-1 protein was observed in both groups, but higher expression areas were observed in iPRF+DBBM group (**Figure 3E**, **3F**).

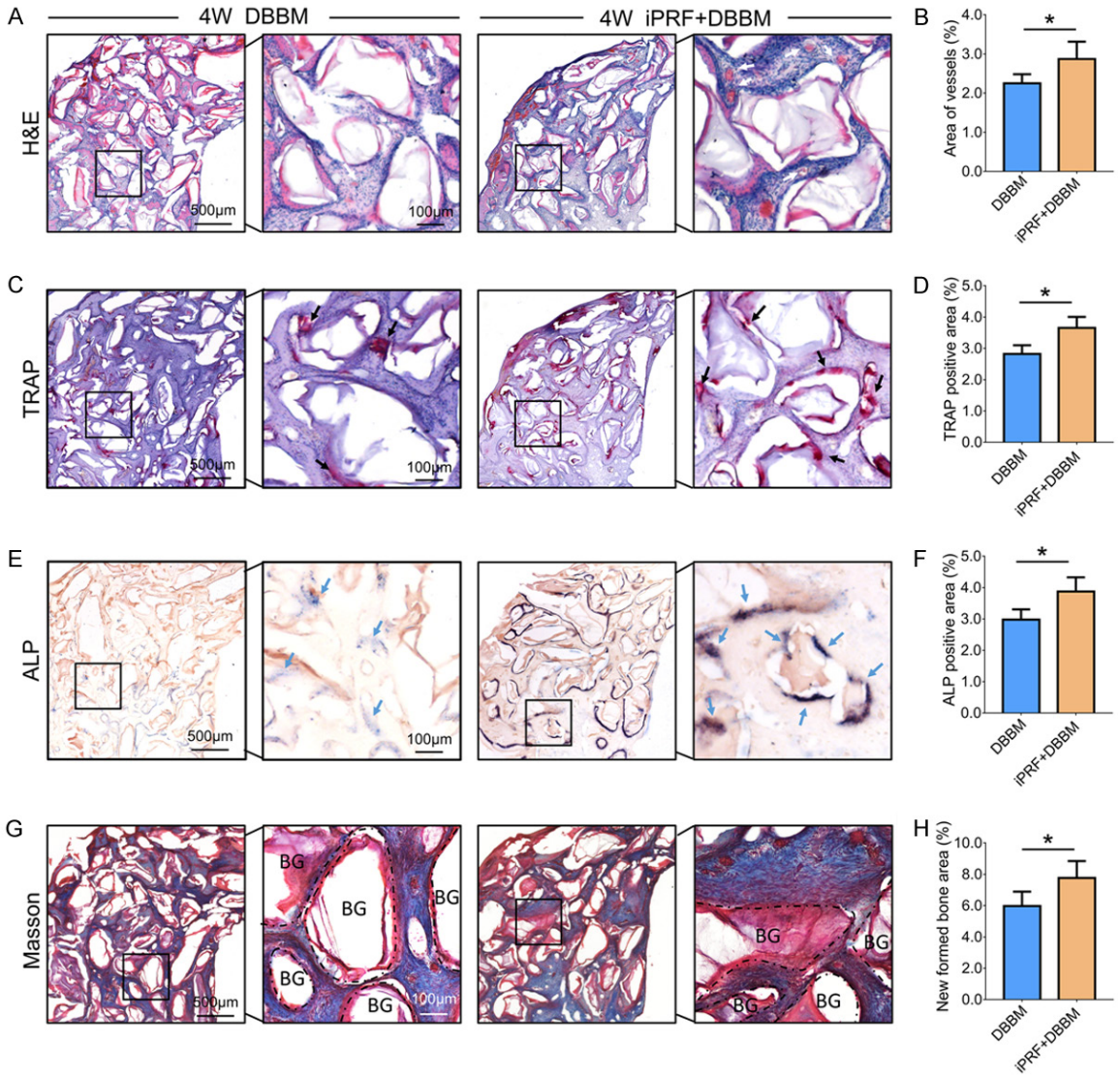

Figure 4. A, C, E, G. H&E staining, TRAP staining, ALP staining and Masson staining images in DBBM region of DBBM and iPRF+DBBM groups after 4 weeks. B, D, F, H. Semiquantitative analysis of vascular formation (white arrow), TRAP positive cells (black arrow), ALP positive cells (blue arrow) and new bone formation in both groups after 4 weeks. In the image of Masson staining, the red color represents host bone or newly formed calcified bone and osteoid tissues while the blue color indicates fibrous tissue or freshly formed bone (n = 4). *$P < 0.05$.

Bone remodeling activity

H&E staining indicated that more vessels were found in the iPRF+DBBM group (**Figure 4A**, **4B**). TRAP staining and ALP staining showed the consistent trend that osteogenic and osteoclastic activity in experimental group is much higher than that of DBBM group. The positive region of ALP and TRAP indicated that large amounts of osteoblasts and osteoclasts occurred surrounding the neovascularization region (**Figure 4C-F**). MT-stained bone specimens showed that immature collagen was dominating in DBBM group with limited areas of mature collagen at 4 weeks postoperatively. However, detectable red stained areas were observed in iPRF+DBBM groups with apparently reduced blue stained areas of immature collagen (**Figure 4G**). Newly formed immature bone in DBBM and iPRF+DBBM groups analyzed by new formed bone area percentage (%) is presented in **Figure 4H**. The ratio of new bone formation in iPRF+DBBM group was 1.3 times higher than that of the DBBM group at 4 weeks postoperatively.

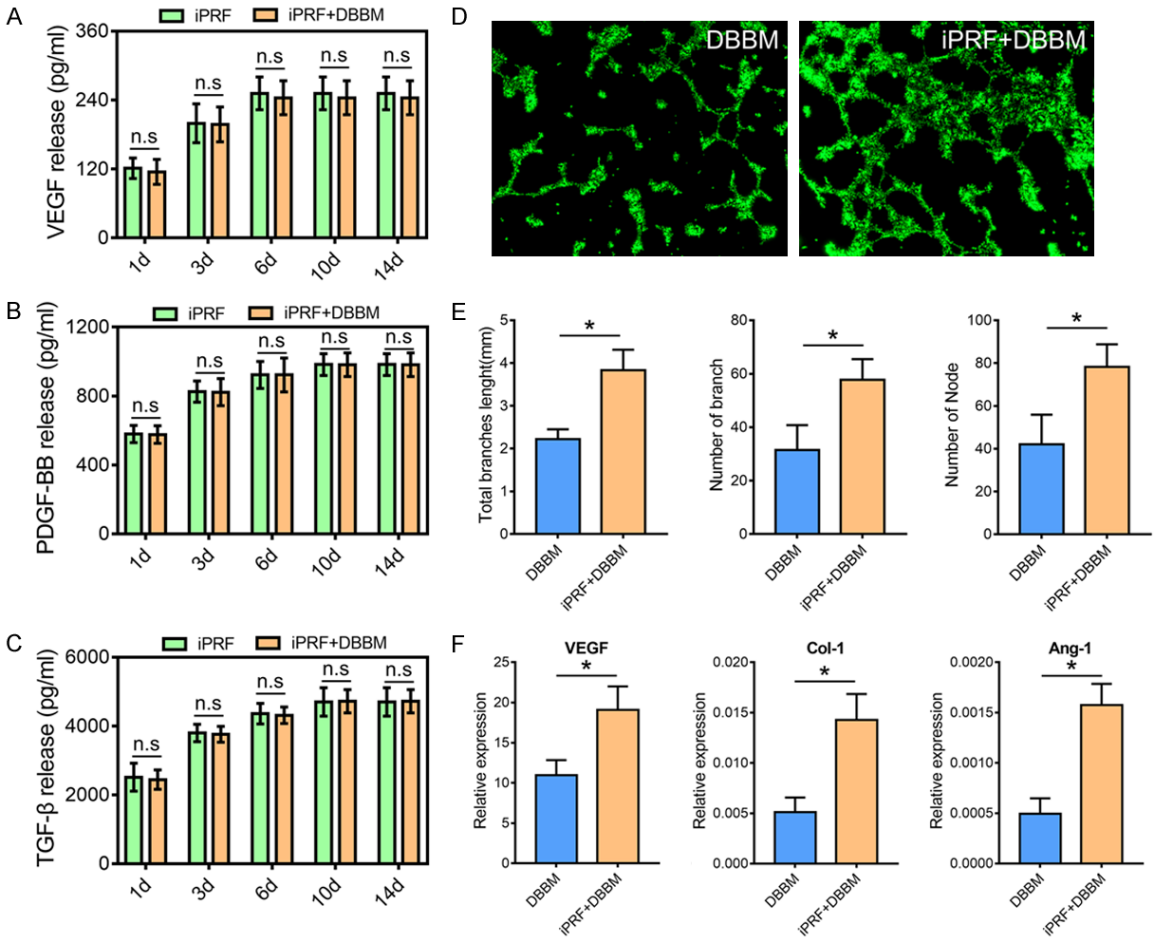

Figure 5. A-C. ELISA results showed the release pattern of three important growth factors (VEGF, PDGF-BB, TGF-β) within iPRF and iPRF+DBBM, respectively (n = 3). D, E. Laser confocal microscope photographs and semiquantitative analysis of tube formation assay showed the promotion of angiogenesis in iPRF+DBBM group (n = 3). F. The qRT-PCR results indicated the mRNA expression of vascular-related genes (n = 3).

Neovascularization

According to result of ELISA, during the setting time-point, the three major growth factors in both groups maintained a prolonged release pattern for nearly 2 weeks (**Figure 5A-C**). This shows that DBBM did not stop the release of factors from iPRF. These growth factors are closely related to angiogenesis and vascular maturation [14]. qRT-PCR and vascular tube formation assay were conducted to verify the angiogenic property of iPRF+DBBM. The results of tube formation revealed that the number of tubes and tube nodes as well as the total tube lengths in the iPRF+DBBM group were totally greater than those in the DBBM group, which further indicated strong angiogenic capacity within iPRF+DBBM group (**Figure 5D**, **5E**). The qRT-PCR results showed that the mRNA levels of *VEGF*, *Col-1* and *Ang-1* were significantly higher in the iPRF+DBBM group compared with the DBBM group (**Figure 5F**).

Discussion

According to the 5th EAO Consensus Conference, the application of PRP and PRF combined with grafting materials in SFA seems not to be recommendable because of a lack of effect [13]. However, the dynamic bone formation pattern has not been observed carefully in previous studies during the early healing process of sinus augmentation. Indeed, for long-term effect on bone regeneration, it seemed that the additional benefit of osteogenic property to increase bone volume is not obvious (**Figure 2A**, **2B**). In the study of kilic et al., they compared the histologic and histomorphometric

outcomes of maxillary sinus-floor augmentation among beta-tricalcium phosphate (β-TCP) alone, P-PRP-mixed β-TCP, and PRF-mixed β-TCP in 26 patients. Their findings suggested that adding P-PRP or PRF to β-TCP graft substitute was not beneficial on new bone formation and regeneration, and P-PRP plus β-TCP or PRF plus β-TCP is not superior to β-TCP alone [22]. Our results seemed not consistent with this study, but we have to take into account of different research models, observation periods and biomaterials between both studies. In our study, iPRF+DBBM could facilitate the early establishment of neovascularization in the maxillary sinus (**Figure 4A**, **4B**) and accelerate bone remodeling process (**Figure 4**). Compared to DBBM, β-TCP is featured by faster degradation and higher substitution rate and it facilitates the bone remodeling process in the experiment of ridge preservation [23, 24], which may also occurred in maxillary sinus elevation. Nevertheless, the slower degradation property of DBBM applied in our study may retard the replacement of new bone formation and the actual bone-regeneration capacity of iPRF. Another study published recently was to investigate the effectiveness of adding leukocyte and platelet-rich fibrin (L-PRF) to DBBM for early implant placement after maxillary sinus augmentation of 12 patients. The results showed that the addition of L-PRF to the DBBM into the maxillary sinus allowed early implant placement (4 months) with increased new bone formation than DBBM alone after 8 months of healing [6]. Our study also suggested that the accelerated process of bone remodeling may allow the early implant placement after sinus augmentation. The alternation of bone remodeling pattern and bone maturation shown in histological results inspired us that there might be some differences after the application of iPRF.

It is widely acknowledged that in the process of bone regeneration, relative biological events include coagulation, inflammatory response, angiogenesis, and accompanying target actions of cell differentiation and mineralization [25]. After a perfect performance of SFA, the grafted biomaterial can be well restrained between bone walls and SM. Blood clots are crucial for postoperative healing since the blood clots will be replaced by organized connective tissues and contributed to the dynamics of later bone remodeling [26]. During the first two weeks, blood clots are evident on the graft bed, which is the focus of the inflammatory response characterized by vascular buds infiltrating the grafted bed. Afterwards, fibrous granulation tissue becomes increasingly dominant on the graft bed, the number of inflammatory cells decreases, and osteoclastic activity increases [26]. Subsequently, grafting material may be covered with vascular network. As the revascularization process proceeds, primitive mesenchymal cells differentiate into osteogenic cells. These osteogenic cells first differentiate into osteoblasts, which line the edges of grafts and deposit one layer of osteoid surrounding the bone grafts. Meanwhile, bone grafts are gradually resorbed by osteoclasts [27]. Using a rabbit sinus model, our study found that loading iPRF onto DBBM particles with soaking method enhanced the osteogenic potential of the SM. The dual direction of bone formation in SFA is believed to accelerate the substitution of bone grafting material and promote bone maturation in early bone healing period (**Figure 3A**, **3B**).

Chemotactic process is the first important step for bone healing [21, 28]. Growth factors within iPRF such as PDGF and TGF-β cause chemotaxis of pre-osteoblasts to sites where bone remodeling is needed, and the chemotactic process is followed by osteogenic proliferation and differentiation. Such growth factors may further orchestrate SDF-1, which has been considered as the most important chemokine [29, 30]. The binding of SDF-1 to CXCR4 results in cytoskeleton rearrangements and integrin activation. This SDF-1/CXCR4-orientated chemotaxis modulates the recruiting of stem cells and progenitor cells [31]. As is shown in **Figure 3E**, crucial chemokines SDF-1 for cell recruitment were apparently observed beneath the SM, which further promote new bone formation in these areas. Moreover, the Transwell assay in vitro also indicated that the migration of pre-osteoblast in iPRF+DBBM group was enhanced due to effect of growth factors (**Figure 3C**, **3D**).

Subsequently, vascular formation surrounding DBBM region was enhanced by molecular factors within iPRF as well [15]. The adequate blood supply that transport nutrients, oxygen and minerals would lay a foundation for bone healing [32]. Consistent with previous study, iPRF+DBBM presented higher potential of vascular formation at 4 weeks according to histomorphometric result of tube forming experi-

ment (**Figure 5D**, **5E**). iPRF contains a variety of autologous factors which affect both intravascular cells and bone-related lineage, emphasizing that the processes of angiogenesis and osteogenesis are interacted [32]. Among these factors, representative growth factors that have been tested are VEGF, PDGF-BB and TGF-β (**Figure 5A-C**), which help stimulate the proliferation of new blood vessels. VEGF mainly promotes vascular formation through recruiting endothelial cells and forming tubules [26]. Moreover, PDGF-BB within iPRF was verified its promotion for the angiogenesis of endothelia progenitor cells and mesenchymal stem cells through PI3K/Akt signaling pathway [33]. Additionally, TGF-β signaling contributes to development of vascular formation by enhancing vascular smooth muscle cell (VSMC) proliferation [34]. Our results showed that iPRF+DBBM could release multiple growth factors in a sustainable pattern for nearly 2 weeks, which facilitated the temporal-spatial vascular formation for new bone formation (**Figure 5A**). Ang-1 is another indicator of angiogenesis. Ang-1 plays a critical role in the acceleration of vascular maturation, which also promote the stabilization and growth of endothelial cells [35]. iPRF+DBBM potentiating neovascularization were verified by detection of early (*VEGF, Col-1*) and late indicators (Ang-1) (**Figure 5F**). Also of note, by antigen presentation and innate immunity, the presence of DBBM would create a slight inflammatory environment [36]. After inflammation altered into the repair stage where mature monocyte/macrophage differentiated into osteoclast, osteoclast would perform normal physiological functions and initiated bone remodeling process. Neovascularization can enhance recruitment of mononucleated preosteoclasts deriving from bone marrow. These preosteoclasts will finally mature into multinucleated osteoclasts for bone resorption [37]. In addition, a variety of growth factors contained in iPRF can directly induce the formation of osteoclasts. For instance, PDGF-BB plays an extremely complex role in bone remodeling and bone regeneration [38]. Previous studies mainly focused on the effect of PDGF-BB on homing of osteogenic and angiogenic progenitor cells, and osteoblast proliferation and differentiation [39, 40]. However, recently some researchers found that PDGF-BB enhances osteoclast formation and osteoclastic bone resorption in vitro and vivo [38, 41]. The newly formed pre-osteoclasts secrete PDGF-BB to further amplify this effect [42]. In addition, TGF-β and IGF-1 can be used as RANKL substitutes to induce osteoclast differentiation through non-canonical Pathways [43-45]. Therefore, higher osteoclast activity was shown in iPRF+DBBM group while less observed in DBBM group (**Figure 4C**, **4D**).

Angiogenesis is considered to be one of the most important driven forces in tissue-healing process [46]. Vascularization can promote bone regeneration by enhancing the differentiation of infiltrating precursor cells of osteoblasts and osteoclasts during new bone formation [46]. Consistent with the result of our study, iPRF+DBBM group showed that abundant formation and active function of osteoblasts and osteoclasts occurred along with the emergence of large number of vascular vessels (**Figure 4A**, **4B**). Specifically, there were more positive signals representing osteogenesis and bone resorption at early healing stage (4^{th} week) in iPRF+DBBM group with more vascular formation (**Figure 4**). Ultimately, the accelerated bone remodeling process will lead to a relative mature bone formation even in a short-term period. With neovascularization and increased number of osteoblasts and osteoclasts under the assistance of iPRF, the active process of bone remodeling will finally contribute to the maturation of bone in early period [6, 15]. As shown in **Figure 4G**, DBBM areas with increased matured collagen appeared red in iPRF+DBBM group indicated that iPRF can promote mature bone formation after 4 weeks.

Overall, this study indicated that iPRF combined with DBBM particles are recommended to use in SFA while iPRF+DBBM stimulates the early angiogenesis and osteogenesis, hence reaching to the subsequent rapid substitution of bone grafting material and faster bone remodeling process, which provides a favorable environment for the ultimate purpose of implantation. Even though the addition of iPRF failed to increase the bone volume among groups, more mature bone structure was observed in the iPRF+DBBM group at early healing period, providing the potential of reducing the interval between bone grafting and implant placement.

Acknowledgements

The authors would like to thank Dr. Li Chen from Analytical & Testing Center Sichuan

University for her help with micro-CT scanning and analysis. This work was supported by the National Nature Science Foundation of China [No. 81701031, 31100690], Postdoctoral Science Foundation of China [No. 2017-M622981], Chongqing Special Postdoctoral Science Foundation [No. XmT2018009] and Chongqing Research Program of Basic Research and Frontier Technology [No. cstc2018jcyjAX0200].

Disclosure of conflict of interest

None.

Address correspondence to: Tao Chen and Yuanding Huang, Stomatological Hospital of Chongqing Medical University, Chongqing Key Laboratory of Oral Diseases and Biomedical Sciences, Chongqing Municipal Key Laboratory of Oral Biomedical Engineering of Higher Education, 426# Songshibei Road, Yubei District, Chongqing 401147, China. Tel: +86-182-2502-9529; E-mail: chentao1985@hospital.cqmu.edu.cn (TC); Tel: +86-136-2831-6711; E-mail: huangyd@hospital.cqmu.edu.cn (YDH)

References

[1] De Santis E, Lang NP, Ferreira S, Rangel Garcia I, Caneva M and Botticelli D. Healing at implants installed concurrently to maxillary sinus floor elevation with Bio-Oss® or autologous bone grafts. A histo-morphometric study in rabbits. Clin Oral Implants Res 2017; 28: 503-511.

[2] Tatum H Jr. Maxillary and sinus implant reconstructions. Dent Clin North Am 1986; 30: 207-229.

[3] Nizam N, Eren G, Akcalı A and Donos N. Maxillary sinus augmentation with leukocyte and platelet-rich fibrin and deproteinized bovine bone mineral: a split-mouth histological and histomorphometric study. Clin Oral Implants Res 2018; 29: 67-75.

[4] Zhang W, Wang X, Wang S, Zhao J, Xu L, Zhu C, Zeng D, Chen J, Zhang Z, Kaplan DL and Jiang X. The use of injectable sonication-induced silk hydrogel for VEGF(165) and BMP-2 delivery for elevation of the maxillary sinus floor. Biomaterials 2011; 32: 9415-9424.

[5] Tadjoedin ES, de Lange GL, Bronckers AL, Lyaruu DM and Burger EH. Deproteinized cancellous bovine bone (Bio-Oss) as bone substitute for sinus floor elevation. A retrospective, histomorphometrical study of five cases. J Clin Periodontol 2003; 30: 261-270.

[6] Pichotano EC, de Molon RS, de Souza RV, Austin RS, Marcantonio E and Zandim-Barcelos DL. Evaluation of L-PRF combined with deproteinized bovine bone mineral for early implant placement after maxillary sinus augmentation: a randomized clinical trial. Clin Implant Dent Relat Res 2019; 21: 253-262.

[7] Schmitt C, Lutz R, Doering H, Lell M, Ratky J and Schlegel KA. Bio-Oss® blocks combined with BMP-2 and VEGF for the regeneration of bony defects and vertical augmentation. Clin Oral Implants Res 2013; 24: 450-460.

[8] Cheng ZA, Alba-Perez A, Gonzalez-Garcia C, Donnelly H, Llopis-Hernandez V, Jayawarna V, Childs P, Shields DW, Cantini M, Ruiz-Cantu L, Reid A, Windmill JFC, Addison ES, Corr S, Marshall WG, Dalby MJ and Salmeron-Sanchez M. Nanoscale coatings for ultralow dose BMP-2-driven regeneration of critical-sized bone defects. Adv Sci (Weinh) 2019; 6: 1800361.

[9] Hong JY, Kim MS, Lim HC, Lee JS, Choi SH and Jung UW. A high concentration of recombinant human bone morphogenetic protein-2 induces low-efficacy bone regeneration in sinus augmentation: a histomorphometric analysis in rabbits. Clin Oral Implants Res 2016; 27: e199-e205.

[10] Masuki H, Okudera T, Watanebe T, Suzuki M, Nishiyama K, Okudera H, Nakata K, Uematsu K, Su CY and Kawase T. Growth factor and pro-inflammatory cytokine contents in platelet-rich plasma (PRP), plasma rich in growth factors (PRGF), advanced platelet-rich fibrin (A-PRF), and concentrated growth factors (CGF). Int J Implant Dent 2016; 2: 19.

[11] Abd El Raouf M, Wang X, Miusi S, Chai J, Mohamed AbdEl-Aal AB, Nefissa Helmy MM, Ghanaati S, Choukroun J, Choukroun E, Zhang Y and Miron RJ. Injectable-platelet rich fibrin using the low speed centrifugation concept improves cartilage regeneration when compared to platelet-rich plasma. Platelets 2019; 30: 213-221.

[12] Miron RJ, Fujioka-Kobayashi M, Hernandez M, Kandalam U, Zhang Y, Ghanaati S and Choukroun J. Injectable platelet rich fibrin (i-PRF): opportunities in regenerative dentistry? Clin Oral Investig 2017; 21: 2619-2627.

[13] Schliephake H, Sicilia A, Nawas BA, Donos N, Gruber R, Jepsen S, Milinkovic I, Mombelli A, Navarro JM, Quirynen M, Rocchietta I, Schiødt M, Schou S, Stähli A and Stavropoulos A. Drugs and diseases: summary and consensus statements of group 1. The 5th EAO Consensus Conference 2018. Clin Oral Implants Res 2018; 29 Suppl 18: 93-99.

[14] Anitua E, Nurden P, Prado R, Nurden AT and Padilla S. Autologous fibrin scaffolds: when platelet- and plasma-derived biomolecules meet fibrin. Biomaterials 2019; 192: 440-460.

[15] Dohle E, El Bagdadi K, Sader R, Choukroun J, James Kirkpatrick C and Ghanaati S. Platelet-

rich fibrin-based matrices to improve angiogenesis in an in vitro co-culture model for bone tissue engineering. J Tissue Eng Regen Med 2018; 12: 598-610.
[16] Wang X, Zhang Y, Choukroun J, Ghanaati S and Miron RJ. Effects of an injectable platelet-rich fibrin on osteoblast behavior and bone tissue formation in comparison to platelet-rich plasma. Platelets 2018; 29: 48-55.
[17] Chen G, Nakamura I, Dhanasekaran R, Iguchi E, Tolosa EJ, Romecin PA, Vera RE, Almada LL, Miamen AG, Chaiteerakij R, Zhou M, Asiedu MK, Moser CD, Han S, Hu C, Banini BA, Oseini AM, Chen Y, Fang Y, Yang D, Shaleh HM, Wang S, Wu D, Song T, Lee JS, Thorgeirsson SS, Chevet E, Shah VH, Fernandez-Zapico ME and Roberts LR. Transcriptional induction of periostin by a sulfatase 2-TGFβ1-SMAD signaling axis mediates tumor angiogenesis in hepatocellular carcinoma. Cancer Res 2017; 77: 632-645.
[18] Mu Z, Chen K, Yuan S, Li Y, Huang Y, Wang C, Zhang Y, Liu W, Luo W, Liang P, Li X, Song J, Ji P, Cheng F, Wang H and Chen T. Gelatin nanoparticle-injectable platelet-rich fibrin double network hydrogels with local adaptability and bioactivity for enhanced osteogenesis. Adv Healthc Mater 2020; 9: e1901469.
[19] Raafat SN, Amin RM, Elmazar MM, Khattab MM and El-Khatib AS. The sole and combined effect of simvastatin and platelet rich fibrin as a filling material in induced bone defect in tibia of albino rats. Bone 2018; 117: 60-69.
[20] Bai Y, Dai X, Yin Y, Wang J, Sun X, Liang W, Li Y, Deng X and Zhang X. Biomimetic piezoelectric nanocomposite membranes synergistically enhance osteogenesis of deproteinized bovine bone grafts. Int J Nanomedicine 2019; 14: 3015-3026.
[21] Hosogane N, Huang Z, Rawlins BA, Liu X, Boachie-Adjei O, Boskey AL and Zhu W. Stromal derived factor-1 regulates bone morphogenetic protein 2-induced osteogenic differentiation of primary mesenchymal stem cells. Int J Biochem Cell Biol 2010; 42: 1132-1141.
[22] Cömert Kılıç S, Güngörmüş M and Parlak SN. Histologic and histomorphometric assessment of sinus-floor augmentation with beta-tricalcium phosphate alone or in combination with pure-platelet-rich plasma or platelet-rich fibrin: a randomized clinical trial. Clin Implant Dent Relat Res 2017; 19: 959-967.
[23] Naenni N, Sapata V, Bienz SP, Leventis M, Jung RE, Hämmerle CHF and Thoma DS. Effect of flapless ridge preservation with two different alloplastic materials in sockets with buccal dehiscence defects-volumetric and linear changes. Clin Oral Investig 2018; 22: 2187-2197.
[24] Ikawa T, Akizuki T, Matsuura T, Hoshi S, Ammar SA, Kinoshita A, Oda S and Izumi Y. Ridge preservation after tooth extraction with buccal bone plate deficiency using tunnel structured β-Tricalcium phosphate blocks: a 2-month histologic pilot study in beagle dogs. J Periodontol 2016; 87: 175-183.
[25] Bayer EA, Gottardi R, Fedorchak MV and Little SR. The scope and sequence of growth factor delivery for vascularized bone tissue regeneration. J Control Release 2015; 219: 129-140.
[26] Shiu HT, Goss B, Lutton C, Crawford R and Xiao Y. Formation of blood clot on biomaterial implants influences bone healing. Tissue Eng Part B Rev 2014; 20: 697-712.
[27] Burchardt H. The biology of bone graft repair. Clin Orthop Relat Res 1983; 28-42.
[28] Wu B, Wang L, Yang X, Mao M, Ye C, Liu P, Yang Z, Yang X, Lei D and Zhang C. Norepinephrine inhibits mesenchymal stem cell chemotaxis migration by increasing stromal cell-derived factor-1 secretion by vascular endothelial cells via NE/abrd3/JNK pathway. Exp Cell Res 2016; 349: 214-220.
[29] Sengupta N, Afzal A, Caballero S, Chang KH, Shaw LC, Pang JJ, Bond VC, Bhutto I, Baba T, Lutty GA and Grant MB. Paracrine modulation of CXCR4 by IGF-1 and VEGF: implications for choroidal neovascularization. Invest Ophthalmol Vis Sci 2010; 51: 2697-2704.
[30] Li Q, Niu Y, Diao H, Wang L, Chen X, Wang Y, Dong L and Wang C. In situ sequestration of endogenous PDGF-BB with an ECM-mimetic sponge for accelerated wound healing. Biomaterials 2017; 148: 54-68.
[31] Zhao Y and Zhang H. Update on the mechanisms of homing of adipose tissue-derived stem cells. Cytotherapy 2016; 18: 816-827.
[32] Jooybar E, Abdekhodaie MJ, Alvi M, Mousavi A, Karperien M and Dijkstra PJ. An injectable platelet lysate-hyaluronic acid hydrogel supports cellular activities and induces chondrogenesis of encapsulated mesenchymal stem cells. Acta Biomater 2019; 83: 233-244.
[33] Rieg AD, Suleiman S, Anker C, Verjans E, Rossaint R, Uhlig S and Martin C. PDGF-BB regulates the pulmonary vascular tone: impact of prostaglandins, calcium, MAPK- and PI3K/AKT/mTOR signalling and actin polymerisation in pulmonary veins of guinea pigs. Respir Res 2018; 19: 120.
[34] Suwanabol PA, Seedial SM, Shi X, Zhang F, Yamanouchi D, Roenneburg D, Liu B and Kent KC. Transforming growth factor-β increases vascular smooth muscle cell proliferation through the Smad3 and extracellular signal-regulated kinase mitogen-activated protein kinases pathways. J Vasc Surg 2012; 56: 446-454.
[35] He Y, Yu X, Chen Z and Li L. Stromal vascular fraction cells plus sustained release VEGF/

Ang-1-PLGA microspheres improve fat graft survival in mice. J Cell Physiol 2019; 234: 6136-6146.

[36] Donos N, Kostopoulos L, Tonetti M, Karring T and Lang NP. The effect of enamel matrix proteins and deproteinized bovine bone mineral on heterotopic bone formation. Clin Oral Implants Res 2006; 17: 434-438.

[37] Søe K, Andersen TL, Hinge M, Rolighed L, Marcussen N and Delaisse JM. Coordination of fusion and trafficking of pre-osteoclasts at the marrow-bone interface. Calcif Tissue Int 2019; 105: 430-445.

[38] Li DQ, Wan QL, Pathak JL and Li ZB. Platelet-derived growth factor BB enhances osteoclast formation and osteoclast precursor cell chemotaxis. J Bone Miner Metab 2017; 35: 355-365.

[39] Friedlaender GE, Lin S, Solchaga LA, Snel LB and Lynch SE. The role of recombinant human platelet-derived growth factor-BB (rhPDGF-BB) in orthopaedic bone repair and regeneration. Curr Pharm Des 2013; 19: 3384-3390.

[40] Demirtaş TT, Göz E, Karakeçili A and Gümüşderelioğlu M. Combined delivery of PDGF-BB and BMP-6 for enhanced osteoblastic differentiation. J Mater Sci Mater Med 2016; 27: 12.

[41] Zhang Z, Chen J and Jin D. Platelet-derived growth factor (PDGF)-BB stimulates osteoclastic bone resorption directly: the role of receptor beta. Biochem Biophys Res Commun 1998; 251: 190-194.

[42] Xie H, Cui Z, Wang L, Xia Z, Hu Y, Xian L, Li C, Xie L, Crane J, Wan M, Zhen G, Bian Q, Yu B, Chang W, Qiu T, Pickarski M, Duong LT, Windle JJ, Luo X, Liao E and Cao X. PDGF-BB secreted by preosteoclasts induces angiogenesis during coupling with osteogenesis. Nat Med 2014; 20: 1270-1278.

[43] Sabokbar A, Mahoney DJ, Hemingway F and Athanasou NA. Non-canonical (RANKL-independent) pathways of osteoclast differentiation and their role in musculoskeletal diseases. Clin Rev Allergy Immunol 2016; 51: 16-26.

[44] Itonaga I, Sabokbar A, Sun SG, Kudo O, Danks L, Ferguson D, Fujikawa Y and Athanasou NA. Transforming growth factor-beta induces osteoclast formation in the absence of RANKL. Bone 2004; 34: 57-64.

[45] Wang Y, Nishida S, Elalieh HZ, Long RK, Halloran BP and Bikle DD. Role of IGF-I signaling in regulating osteoclastogenesis. J Bone Miner Res 2006; 21: 1350-1358.

[46] Sivaraj KK and Adams RH. Blood vessel formation and function in bone. Development 2016; 143: 2706-2715.